Phase diagram of $Bi_{2.15}Sr_{1.85}CaCu_2O_{8+\delta}$ in the presence of columnar defects

D. Zech,* S. L. Lee, and H. Keller
Physik-Institut der Universität Zürich, CH-8057 Zürich, Switzerland

G. Blatter
Theoretische Physik ETH, CH-8093, Zürich, Switzerland

P. H. Kes and T. W. Li
Kamerlingh Onnes Laboratorium, Leiden University, P.O. Box 9506, 2300 RA Leiden, The Netherlands
(Received 30 April 1996)

Using a combination of high-precision torque and SQUID magnetometry we investigate the irreversibility line of single-crystalline $Bi_{2.15}Sr_{1.85}CaCu_2O_{8+\delta}$ defected with irradiation-induced columnar pins. We find that the irreversibility line cannot be identified with a shifted melting line but rather follows the crossover line $B_{rb}(T)$ separating the single-vortex strong pinning regime from the collective weak pinning regime. Good agreement is found with a theoretical analysis accounting for the strong layering of the material. [S0163-1829(96)04834-5]

In high-T_c superconductors the properties of vortices are strongly influenced by thermal fluctuations and quenched disorder. Static disorder due to imperfections gives rise to pinning of the vortex cores, while dynamic fluctuations of the vortex positions lead to thermal depinning and ultimately to vortex-lattice melting (for a review see Ref. 1). In addition to the random disorder from point defects producing isotropic pinning, correlated disorder due to extended defects generated via irradiation with fast heavy ions has recently attracted a great deal of attention. The magnetic phase diagram of vortices in the presence of columnar defects has been studied theoretically by mapping the vortex problem onto a system of two-dimensional (2D) bosons subject to static disorder.[1,2] At low temperatures and for a density of flux lines less than the density of columnar defects ($B<B_\Phi$) a Bose-glass (BG) phase has been predicted, with strong localization of vortices onto the tracks. At higher fields and temperatures the system undergoes a BG transition $B_{BG}(T)$ to an entangled vortex liquid phase. In irradiated $YBa_2Cu_3O_{7-\delta}$ (YBCO), the prototype continuous anisotropic material, this BG transition defining the onset of irreversibility could be successfully interpreted in terms of a melting transition shifted towards higher temperatures and fields as a consequence of pinning.[3,4] The situation is very different in $Bi_{2.15}Sr_{1.85}CaCu_2O_{8+\delta}$ (BSCCO), the prototype layered material with a pronounced two-dimensional character. In this material, the presence of a low density of columnar defects is sufficient to produce a large shift of the irreversibility line (IL) to higher temperatures. Furthermore, the form of this line exhibits features which are not present in the melting line of the pristine material[5–7] and one concludes that the BG transition cannot be obtained in terms of a simple shift of the vortex lattice melting transition.

In this work we study the IL in BSCCO in the presence of columnar defects, using the complementary experimental techniques of SQUID and torque magnetometry, and develop a theoretical interpretation of the resulting BG line in terms of the accommodation field $B_{rb}(T)$ separating the single-vortex strong pinning region from the collective weak pinning regime.

The experiments have been performed on a high-quality single crystal ($T_c \approx 92$ K) (Ref. 8) cut and cleaved into two square plates $1\times1\times0.05$ mm^3, with the crystallographic c direction along the shortest dimension. One of the crystals has been irradiated with 5.8 GeV Pb ions at GANIL (Caen, France) at 45° to c to produce a track density equivalent to a field $B_\Phi = 200$ mT. The irradiation has been performed in this geometry in order to give a nonvanishing torque signal for the field applied parallel to the defects. The chosen measurement configuration then allows us to compare the measurements from both SQUID and torque magnetometry under identical conditions. The IL's have been obtained from magnetization measurements performed with the field B parallel to the defects and using two complementary irreversibility criteria. The irreversibility *temperature* $T_{irr}(B)$ has been determined by resolving the collapse of the field-cooled and zero-field-cooled magnetization using a commercial SQUID magnetometer. SQUID magnetometry is a quasi-dc method, involving large time intervals between changes of temperature and evaluation of the resulting magnetization. The $T_{irr}(B)$ line therefore traces the onset of static irreversibility due to strong pinning of flux lines. Alternatively, we have used a custom-made torque magnetometer to determine the irreversibility *field* $B_{irr}(T)$ where the magnetic hysteresis curves collapse. Torque magnetometry is a dynamic technique, since it is possible to monitor continuously the torque while sweeping the applied field. The $B_{irr}(T)$ line therefore traces the onset of flux-line relaxation which is faster then the characteristic time scale of the torque measurement. The two lines T_{irr} and B_{irr} obtained from the above irreversibility criteria are in general well separated.

Figure 1 displays the IL's of the irradiated sample obtained in the region $B \lesssim B_\Phi$ by SQUID (T_{irr}) and by torque magnetometry [$B^1_{irr}(T)$, $B^{10}_{irr}(T)$] measured for the two sweep

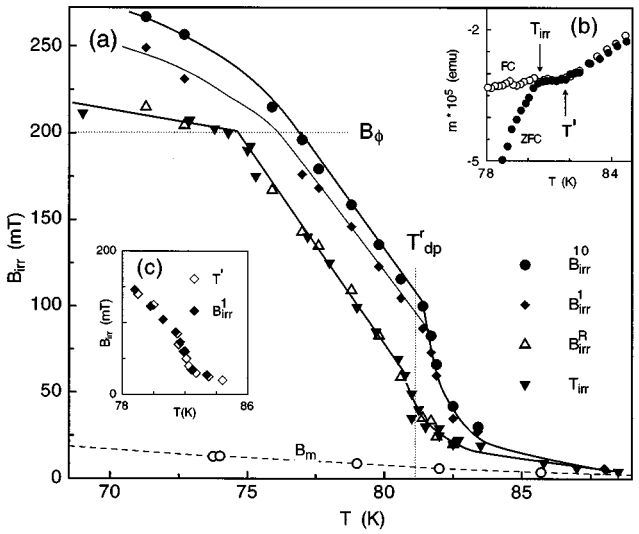

FIG. 1. (a) The irreversibility lines (IL's) of BSCCO with columnar defects. (i) $T_{\rm irr}$ (inverted triangles) obtained from the collapse of field-cooled (FC) and zero-field-cooled (ZFC) SQUID magnetization data. (ii) $B^1_{\rm irr}$ (diamonds) and $B^{10}_{\rm irr}$ (circles) obtained from the collapse of hysteresis loops measured using torque magnetometry at field sweep rates of 1 and 10 mT/s, respectively. (iii) $B^R_{\rm irr}$ (triangles) from the hysteresis loops derived from the relaxed torque signal. (iv) Melting line B_m (open squares) of the unirradiated sample obtained using SQUID magnetometry. The solid and dashed lines are guides to the eye. (b) FC and ZFC magnetization shows an additional feature at $T'>T_{\rm irr}$. (c) The feature T' (open diamonds) lies close to $B^1_{\rm irr}$ (solid diamonds).

rates of 1 and 10 mT/sec, respectively. Also shown is the IL from the relaxed hysteresis loop ($B^R_{\rm irr}$) obtained by sweeping at 10 mT/s and pausing the field at intervals of 2.5 mT for a period of 5 s. First, we note that the IL's $B^1_{\rm irr}$ and $B^{10}_{\rm irr}$ despite a factor of 10 difference in sweep rate, are still closely separated, yet lie well above $B^R_{\rm irr}$. Moreover, it is found that after only a few seconds the IL's $B^R_{\rm irr}$ and $T_{\rm irr}$ coincide. This agreement is particularly noteworthy in view of the very different methods of obtaining the IL's. Whereas for the highest sweep rate the IL approaches the onset of fast flux relaxation, the torque magnetometry in the limit of vanishing sweep rate probes the onset of strong pinning. At low fields $B<B_\Phi$ a pronounced break in curvature at the temperature $T'>T_{\rm irr}$ may be discerned in the SQUID data shown in Fig. 1(b). This feature is found to coincide with the IL $B^1_{\rm irr}$ [see Fig. 1(c)] and reflects the onset of fast flux-line relaxation on the time scale of the SQUID measurement. In the irradiated sample the IL therefore is not a single line but rather a continuous family of lines with a lower boundary $T_{\rm irr}$ which marks the onset of strong pinning and an upper boundary $B^{10}_{\rm irr}$ above which fast flux-line relaxation dominates. Both boundaries are well discerned by the two complementary techniques of SQUID and torque magnetometry. For the pristine reference sample, on the other hand, torque hysteresis measurements show at $B_m(T)$ a jump in the magnetization,[9] signaling a thermodynamic vortex-lattice melting transition.[10,11] For low fields $B<50$ mT the melting line B_m matches exactly the onset of irreversibility and its position is independent of the sweep rate.[9] The IL of the reference sample shown in Fig. 1 is therefore a single line and is further referred as the melting line B_m.

We now turn to the form of the IL of the irradiated sample as given by $B^{10}_{\rm irr}$ but also reflected in the other IL's. The IL is characterized by two key parameters, the matching field B_Φ and the temperature $T^r_{\rm dp}$, which we will identify with the depinning temperature of the BG model in our analysis below. For $T\simeq T^r_{\rm dp}$ and for $B\simeq B_\Phi$ a pronounced kink in the IL is observed which separates the IL into regimes with different temperature dependences. For $T<T^r_{\rm dp}$ the IL is shifted far above B_m and exhibits features not present in the unperturbated melting line of the reference sample. For $T>T^r_{\rm dp}$ the IL drops substantially and for even higher temperatures $T>83$ K the IL's $B^{10}_{\rm irr}$, $B^1_{\rm irr}$, and $T_{\rm irr}$ merge. In this regime the IL of the irradiated sample is only slightly shifted above the melting line B_m of the reference sample. The regime $T\ll T^r_{\rm dp}$ and $B\gg B_\Phi$, in which point disorder and the vortex-vortex interaction competes with the correlated disorder, has been discussed elsewhere.[6]

An interpretation of these experimental findings can be obtained via an analysis of the vortex lattice melting transition in the presence of disorder. We start the discussion with the 3D continuous anisotropic case and then highlight the modifications necessary to describe the 2D layered situation relevant for BSCCO. Also note that in the discussion below we assume the defects to be parallel to the applied field and the c axis. For this simpler case the IL, however, shows the same characteristic features as described above.[6] The system under consideration is characterized by the competition between pinning and thermal fluctuations.

(i) *Pinning* by columnar defects defines a strong pinning region $B<B_{\rm rb}(T)\leqslant B_\Phi$, where all vortices remain trapped onto their pins, despite the presence of thermal fluctuations. At low temperatures, where the track radius r_r exceeds the coherence length ξ, the accommodation field is $B_{\rm rb}\simeq B_\Phi$. Above the temperature $T_{r\xi}$ defined by the relation $\xi(T_{r\xi})=r_r$ (track radius) the accommodation field $B_{\rm rb}(T)$ decreases linearly until at the depinning temperature $T^r_{\rm dp}$ the thermal energy is sufficient to excite vortex segments away from the defects and $B_{\rm rb}\propto\exp(-T/T^r_{\rm dp})$ drops exponentially. Finally, above the delocalization temperature $T_{\rm dl}\gtrsim T^r_{\rm dp}$ the accommodation field is determined by the competition between the lattice elasticity and the collective pinning energy and one obtains $B_{\rm rb}(T)\propto(1-T/T_c)^6$ (Refs. 1 and 2). The position of $B_{\rm rb}$ is essentially characterized by the two parameters B_Φ and $T^r_{\rm dp}$. The dose-equivalent field B_Φ is given by the chosen irradiation dose. On the other hand, the depinning temperature is susceptible to the intrinsic properties of the vortex lines. Within the continuous elastic description we estimate $T^r_{\rm dp}\approx\xi\sqrt{\epsilon_l\epsilon_r}$, where $\epsilon_l\approx\epsilon^2\epsilon_0$, and $\epsilon_r\approx\alpha\epsilon_0$ denote the elastic line tension and the pinning energy, respectively. The basic energy scale is given by the line energy $\epsilon_0=(\Phi_0/4\pi\lambda)^2$, $\epsilon<1$ is the effective mass anisotropy, and $\alpha<1$ is the pinning efficiency of the columnar tracks. For a layered material the depinning temperature is given by $T^r_{\rm dp}\approx d\epsilon_r$, with d the layer thickness.

(ii) In a clean material the *thermal fluctuations* trigger a (first-order) melting transition at $B_m(T)$. In the presence of disorder, this transition is shifted to higher temperatures and fields and turns into a (second-order) BG transition $B_{\rm BG}(T)$. Depending on the relative importance of quenched disorder and thermal fluctuations, the accommodation field

$B_{\rm rb}(T)$ can end up either below or above the melting line $B_m(T)$. As we will show below, the position of the Bose glass or irreversibility line strongly depends on the relative position of $B_{\rm rb}$ and B_m.

Following Nelson and Vinokur[2] (see also Refs. 1, 3, and 12), we consider an individual vortex line in the cage of its neighbors. The usual Lindemann melting criterion $\langle u^2\rangle = c_L^2 a_0^2$ can be transcribed into the condition $T = \epsilon_{\rm elast} = c_L^2 c_{66} a_0^2 L_T$; i.e., the lattice melts when the thermal energy matches the fraction c_L^2 of the cage energy $c_{66} a_0^2 L_T$. Here, c_{66} is the shear modulus, c_L is the Lindemann number, and the longitudinal length $L_T = \epsilon a_0$ follows from the competition between shear and tilt energies. In the presence of disorder, we obtain the position of the irreversibility line by accounting for the (collective) pinning energy $\epsilon_{\rm pin} = L_T \sqrt{\epsilon_r^2 b_0^4 / d_r^2 \langle u^2\rangle}$ of the caged vortex line in the generalized criterion $T = \epsilon_{\rm elast} + \epsilon_{\rm pin}$. Here, d_r denotes the mean track distance and $b_0 = \max(r_r, \sqrt{2}\xi)$. In the perturbative approach used in Ref. 3 one assumes that disorder introduces merely a small shift of the melting line $T_m(B)$. Using the Lindemann criterion $\langle u^2\rangle = c_L^2 a_0^2$ in the expression for $\epsilon_{\rm pin}$ one obtains the result

$$T_{\rm BG}(B) = \gamma T_m(B) + (1-\gamma) T_{c2}(B), \tag{1}$$

with $\gamma \approx 1/[1 + (r_r/d_r)(T_{\rm dp}^r/T_c)]$. This approach has been successfully applied to describe the IL in irradiated YBCO; see Refs. 3 and 4. It assumes that at the glass transition the elastic energy is the dominant energy in the vortex system; hence $B_{\rm rb} < B_m$. This assumption breaks down for strong pinning in a very soft lattice, where the individual vortices remain pinned to their tracks even at temperatures and fields above the melting line B_m and thus $B_m < B_{\rm rb}$. We then neglect the elastic contribution in our irreversibility criterion and obtain the condition $T = \epsilon_{\rm pin}(\langle u^2\rangle(T))$. Using the 3D expression for $\langle u^2\rangle(T) \simeq T a_0/\epsilon\epsilon_0$ we obtain, up to logarithmic accuracy, the result

$$B_{\rm BG}(T) \simeq B_\Phi \frac{\epsilon_r}{\epsilon_0} \left(\frac{b_0}{d_r}\right)^2 \left(\frac{T_{\rm dl}}{T}\right)^6. \tag{2}$$

This expression for the Bose-glass transition line exactly matches the result $B_{\rm rb}$ for the accommodation field in the high-temperature regime $T > T_{\rm dl}$; see Ref. 1. We obtain the result that melting occurs immediately upon entering the collective pinning regime, where the elastic energy becomes of equal importance as the pinning energy, and the resulting vortex liquid is homogeneous (note that at $B_{\rm rb}$ the collective pinning radius $R_c \simeq a_0$). Below $T_{\rm dl}$ the pins are very efficient in reducing the fluctuations of the vortices at fields $B < B_{\rm rb}$; i.e., $\langle u^2\rangle_{\rm sv} = \xi^2 (T/T_{\rm dp}^r)^2 \exp(T/T_{\rm dp}^r)$ for $T_{\rm dp}^r < T < T_{\rm dl}$, and $\langle u^2\rangle_{\rm sv} = \min(\xi^2, r_r^2)$ for $T < T_{\rm dp}^r$. As a consequence the vortex system cannot melt any more. Increasing the field above $B_{\rm rb}$ at temperatures $T < T_{\rm dl}$ we obtain two classes of vortices, those strongly pinned to their associated tracks and the remaining ones in between the pins forming a liquid state. We thus identify the IL with the accommodation field $B_{\rm rb}$ even below the delocalization temperature $T_{\rm dl}$. The resulting vortex liquid is inhomogeneous with a fraction of the flux lines remaining localized on the columnar tracks. The boundary between the homogeneous and the inhomogeneous liquids can be obtained from the condition $\langle u^2\rangle_{\rm sv} = \langle u^2\rangle$ (we use $\langle u^2\rangle$ as an estimate of the short-time–short-range fluctuations in the liquid)

$$B_x = B_\Phi \frac{d_r^2}{\xi^2} \frac{\epsilon_r}{\epsilon_0} \left(\frac{T_{\rm dp}^r}{T}\right)^2 \exp\left(-\frac{2T}{T_{\rm dp}^r}\right), \tag{3}$$

rising steeply for $T_{\rm dp}^r < T < T_{\rm dl}$. Finally, the IL goes over into the melting line of the unirradiated material as the latter increases above the matching field $B_{\rm rb}$; see Fig. 2. The above analysis applies to a 3D continuous anisotropic superconductor with strong pinning. The strongly layered BSCCO material is better described by a 2D model. In this case, the depinning and delocalization temperatures collapse and the single-vortex strong pinning regime terminates abruptly at the 2D depinning temperature $T_{\rm dp}^r = \alpha d \epsilon_r$, where d denotes the layer thickness. Above $T_{\rm dp}^r$ pinning is weak and the perturbative approach should hold, with the Bose-glass line described by Eq. (1). Below $T_{\rm dp}^r$ the glass line follows the accommodation field $B_{\rm rb}$ up to fields $B \simeq B_\Phi$ and then approaches the melting line of the pristine material at low temperatures and high fields $B > B_\Phi$. The line separating the homogeneous liquid from the inhomogeneous one is determined by the field-independent depinning temperature $T_{\rm dp}^r$. Sketches of the resulting phase diagram for the 3D and 2D situations are shown in Fig. 2.

Comparing our experimental findings with the above analysis we identify the measured IL with the accommodation field $B_{\rm rb}(T)$. The first kink at $T = 75$ K, $B = B_\Phi$, we identify with the crossover temperature $T_{r\xi}$ where the track radius matches up with the coherence length $\xi(T)$. Using typical estimates for $\xi(0) \simeq 25$ Å and $r_r \simeq 35$ Å (see Ref. 13) we find $T_{r\xi} = 77$ K, in good agreement with our experiment. Second, we identify the sharp feature at $T = 81$ K with the depinning temperature $T_{\rm dp}^r$. Using typical parameters for BSCCO ($d = 15$ Å, $\lambda = 1800$ Å, and $T_c = 92$ K) and a pinning efficiency of $\alpha = 1$ we obtain $T_{\rm dp}^r = 84$ K. For a more realistic value of $\alpha = 0.7$ we obtain $T_{\rm dp}^r = 81$ K, in good agreement with the position of the sharp drop in our measured irreversibility line. Moreover, above the depinning temperature $T_{\rm dp}^r \simeq 81$ K pinning is largely reduced and the IL drops substantially. Previously we have shown that in this temperature regime the pinning properties of the defects become increasingly isotropic.[6] This implies that the flux lines are no longer strongly localized onto the defects. As a consequence, the weak pinning in this regime can be treated as a perturbation and the IL is well described by the perturbated melting line given in Eq. (1).

Summarizing, we have experimentally traced the irreversibility line in irradiated BSCCO single crystals using high-precision torque and SQUID magnetometry. We identify the measured IL with the Bose-glass transition of the vortex system and find that the latter is shifted far above the melting line of the pristine material. We have presented theoretical estimates for the position of the IL using a generalized Lindemann criterion which accounts for the presence of pinning. We have identified two possible scenarios: (i) For $B_{\rm rb} < B_m$ (weak pinning, hard lattice) the disorder energy is a small correction to the main elastic energy in the vortex system and the BG line is perturbatively shifted with respect to the

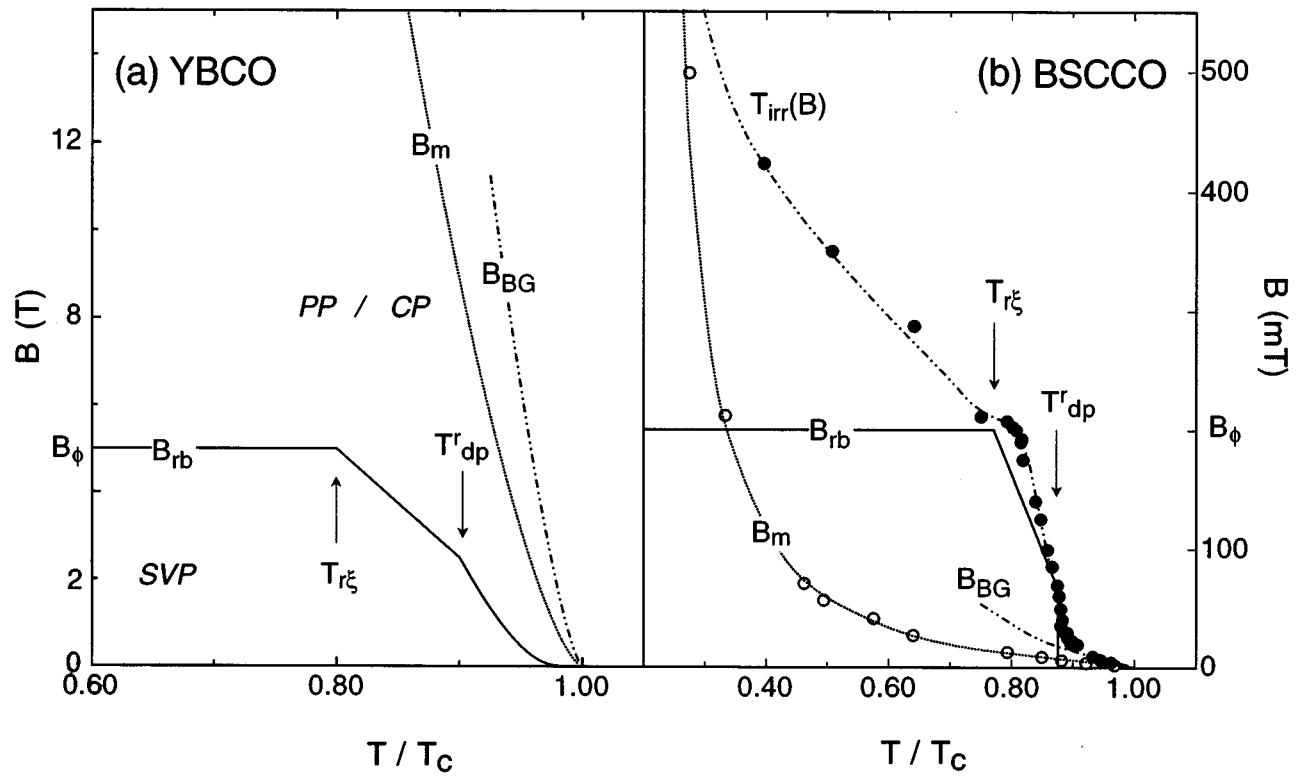

FIG. 2. Schematic representations of the magnetic phase diagram for the 3D continuous anisotropic and 2D layered cases in the presence of columnar defects. The line $B_{\rm rb}$ represents the crossover from the single-vortex (SVP) to plastic/collective (PP/CP) pinning regime. The characteristic temperatures $T_{r\xi}$ and $T^r_{\rm dp}$ are defined in the text. (a) The approximate form of $B_{\rm rb}$ using typical material parameters for YBCO with a $B_\Phi = 5$ T. Note that B_m resides *above* $B_{\rm rb}$, so that one may deduce the Bose-glass melting line $B_{\rm BG}$ using a perturbative approach. (b) $B_{\rm rb}$ using typical material parameters for BSCCO with $B_\Phi = 200$ mT. Note that this line abruptly ends at $T^r_{\rm dp}$. The measured IL's for the irradiated sample $T_{\rm irr}$ (solid circles) and unirradiated sample B_m (open circles) are also included. Note how in this case B_m cuts $B_{\rm rb}$ at low temperatures, such that it lies well *below* $B_{\rm rb}$ for $T \lesssim T^r_{\rm dp}$ Only for $T > T^r_{\rm dp}$ the Bose-glass line $B_{\rm BG}$ is described using a perturbative approach.

melting line. (ii) For $B_{\rm rb} > B_m$ (strong pinning and soft lattice) the IL matches the accommodation field $B_{\rm rb}$ at low fields and approaches the pristine material's melting line at high fields. Comparison of our experimental and theoretical results shows that irradiated BSCCO follows the second type of behavior. Identifying the kinks in the IL at $T = 75$ K and $T = 81$ K with $T_{r\xi}$ and $T^r_{\rm dp}$ and the plateau at $B = 200$ mT with B_Φ, we obtain good quantitative agreement between our experimental data and the theoretical analysis.

We wish to thank M. Konczykowski for supplying us with irradiated samples of BSCCO using the facilities kindly provided by GANIL (Caen, France). This work was supported by the Swiss National Science Foundation (NFP30 No. 4030-32785).

*Present address: Ginzton Laboratory, Stanford University, Stanford, CA 94305.

[1] G. Blatter, M. V. Feigel'man, V. B. Geshkenbein, A. I. Larkin, and V. M. Vinokur, Rev. Mod. Phys. **66**, 1125 (1994).

[2] D. R. Nelson and V. M. Vinokur, Phys. Rev. Lett. **68**, 12 398 (1992); Phys. Rev. B **48**, 13 060 (1993).

[3] L. Krusin-Elbaum, L. Civale, G. Blatter, A. D. Marwick, F. Holtzberg, and C. Feild, Phys. Rev. Lett. **72**, 1914 (1994).

[4] A. V. Samoilov and M. Konczykowski, Phys. Rev. Lett. **75**, 186 (1995).

[5] V. Hardy, Ch. Simon, J. Provost, and D. Groult, Physica C **205**, 371 (1993).

[6] D. Zech, S. L. Lee, H. Keller, G. Blatter, B. Janossy, P. H. Kes, and T. W. Li, Phys. Rev. B **52**, 6913 (1995).

[7] C. J. van der Beek, M. Konczykowski, V. M. Vinokur, T. W. Li, P. H. Kes, and G. W. Crabtree, Phys. Rev. Lett. **74**, 1214 (1995).

[8] T. W. Li, P. H. Kes, N. T. Hien, J. J. M. Frane, and A. A. Menovsky, J. Cryst. Growth **135**, 481 (1994).

[9] D. Zech, M. Willemin, C. Rossel, J. Hofer, and H. Keller (unpublished).

[10] S. L. Lee, P. Zimmermann, H. Keller, M. Warden, I. M. Savic, R. Schauwecker, D. Zech, R. Cubitt, E. M. Forgan, P. H. Kes, T. W. Li, A. A. Menovsky, and Z. Tarnawski, Phys. Rev. Lett. **71**, 3862 (1993).

[11] E. Zeldov, D. Majer, M. Konczykowski, V. B. Geshkenbein, V. M. Vinokur, and H. Shtrikman, Nature **375**, 373 (1995).

[12] A. I. Larkin and V. M. Vinokur, Phys. Rev. Lett. **75**, 4666 (1995).

[13] V. Hardy, J. Provost, D. Groult, M. Hervieu, B. Raveau, S. Durčok, E. Pollert, J. C. Frison, J. P. Chaminade, and M. Pouchard, Physica C **191**, 85 (1992).